THE OFFICIAL MAGAZINE OF THE OCEANOGRAPHY SOCIETY

Oceanography

CITATION

Sarkar, S., H.T. Pham, S. Ramachandran, J.D. Nash, A. Tandon, J. Buckley, A.A. Lotliker, and M.M. Omand. 2016. The interplay between submesoscale instabilities and turbulence in the surface layer of the Bay of Bengal. *Oceanography* 29(2):146–157, http://dx.doi.org/10.5670/oceanog.2016.47.

DOI

http://dx.doi.org/10.5670/oceanog.2016.47

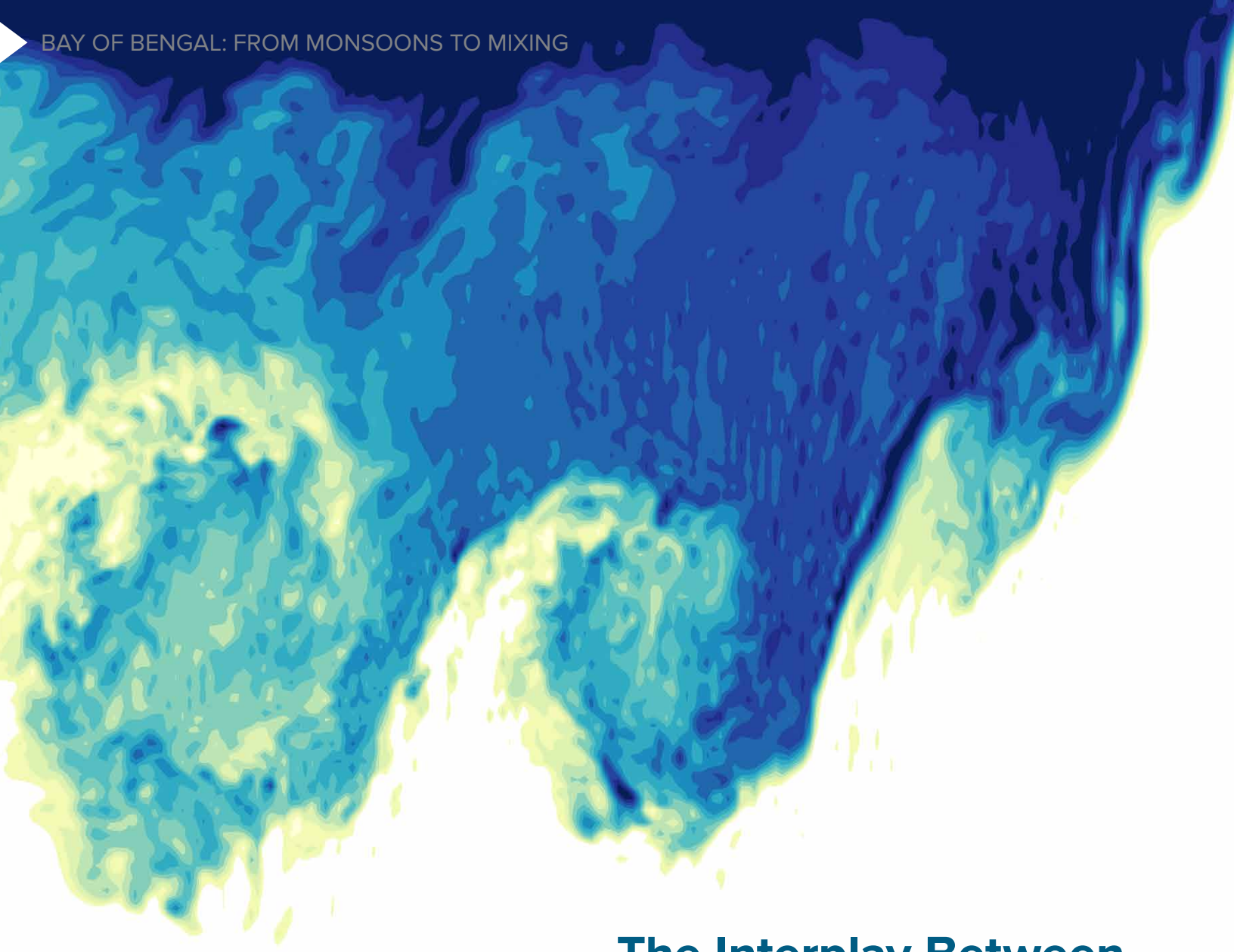

The Interplay Between Submesoscale Instabilities and Turbulence in the Surface Layer of the Bay of Bengal

By Sutanu Sarkar, Hieu T. Pham, Sanjiv Ramachandran, Jonathan D. Nash, Amit Tandon, Jared Buckley, Aneesh A. Lotliker, and Melissa M. Omand

ABSTRACT. The Air-Sea Interactions Regional Initiative (ASIRI) aims to understand vertical fluxes of momentum and heat across the surface layer in the Bay of Bengal. As the mesoscale and submesoscale eddies redistribute freshwater input over saline water of the bay, they influence the vertical distribution of salinity and thus impact air-sea fluxes. This study reports on numerical simulations performed to investigate processes that can lead to the observed vertical structure of stratification near the ocean surface. Processes are explored at multiple lateral scales, ranging from a few meters to tens of kilometers, to elucidate how the interplay among large-scale motion, submesoscale instabilities, and small-scale turbulent motion affects the surface layer.

INTRODUCTION

The Arabian Sea and the Bay of Bengal (BoB) span similar latitudes in the northern Indian Ocean. However, the Bay of Bengal is a low-salinity basin compared to the Arabian Sea, due to freshwater fluxes into the bay from summer and winter monsoon precipitation and riverine inputs (Gordon et al., 2016, in this issue). Oceanic mesoscale eddies of O(100 km) stir the freshwater input into sharp frontal gradients of O(1–10 km) with relatively shallow mixed layers of a few meters; these fronts interact with monsoonal wind forcing and lead to instabilities and vertical mixing. Upper-ocean salinity stratification in the BoB is therefore set by a complex interplay of multidimensional processes at submesoscales as well as smaller scales. The upper-ocean stratification in turn modulates the air-sea fluxes at various spatiotemporal scales and thereby influences the monsoons.

Exploration of mid-latitude upper-ocean submesoscale variability includes observations and models of the north wall of the Gulf Stream in the North Atlantic during the Scalable Lateral Mixing and Coherent Turbulence (LATMIX) experiments (Shcherbina et al., 2015). LATMIX observations, advancements in related theory, and process simulations reveal much about submesoscale instabilities in mid-latitudes. Instabilities are generated at a variety of scales and are fueled by different mechanisms; for example, available potential energy is released to the instability motion in the case of ageostrophic baroclinic instability (e.g., Fox-Kemper et al., 2008), and kinetic energy is released in the case of symmetric instability (e.g., Taylor and Ferrari, 2010). The resulting submesoscale motions in models affect upper-ocean dynamics, thermodynamics, and biogeochemistry through their direct impact on vertical buoyancy fluxes that restratify the upper ocean and also impact mixing. Recent studies have shown that the magnitude of the horizontal frontal gradient as well as the depth of the mixed layer directly affect the vertical buoyancy flux driven by ageostrophic baroclinic instability of upper-ocean frontal gradients (Fox-Kemper et al., 2008). These submesoscale motions are important for the Bay of Bengal because recent measurements show that the bay has a shallow mixed layer and is replete with buoyancy gradients arising from large salinity gradients.

Mesoscale strain and wind act on freshwater river input and precipitation to create salinity gradients over a wide range of horizontal scales in the BoB, leading to frontal zones ranging from over tens of kilometers to unusually sharp salinity contrasts over a distance of a few meters. Furthermore, frontal zones are susceptible to a variety of flow instabilities. Figure B1 shows three examples of observed fronts in the Bay of Bengal that exhibit differing degrees of sharpness. The variability of salinity with horizontal and vertical gradients over a wide range of scales is remarkable.

Here, we seek to elucidate mechanisms that set up stratification in the BoB at multiple scales (see Box 1). In the following sections, we describe results from numerical models that help us understand the dynamics associated with each of these examples. When the frontal zone is strong as in Figure B1(b,c), the scale of the nonlinearly evolving lateral instabilities becomes small and couples strongly with vertical processes so that three-dimensional instabilities become integral to its evolution. Here, large eddy simulation (LES) with an adaptive model for subgrid dynamics is used to examine such a strongly coupled situation with sufficiently high resolution (order meter in the horizontal and finer in the vertical) so that the energetic three-dimensional turbulent motions and the forward cascade from unforced submesoscale instabilities are resolved. For the case of moderate frontal strength, the lateral processes have much larger horizontal scales than those of vertical mixing processes. We then examine the role of stirring by submesoscale instabilities in setting the stratification structure when a large-scale front responds to wind and thermal forcing. A nonhydrostatic solver with a resolution of 1 km in the horizontal is used to permit submesoscale instabilities and, instead of resolving three-dimensional turbulence, a one-dimensional turbulent mixing model is employed as a simplification.

NONLINEAR BORES AND TURBULENCE

Thin ~O(10 m), highly nonlinear internal bores that propagate near the surface and transit through lateral density gradients are found in the Bay of Bengal. Figure B1c shows two realizations of the small-scale salinity changes in the bore observed in November 2013. Ten snapshots of the bore were obtained over a 10 h period, revealing the following characteristics: (1) the bore is driven by a partially compensated horizontal density gradient bringing fresher and cooler water from the south toward the north; (2) sharp salinity and temperature jumps occur over only a few meters in the horizontal; (3) the bore decelerates, rotates, and becomes partially arrested after about eight hours; (4) there is a surface flow convergence ahead of the bore, and the warm saline water subducts into regions below the bore; and (5) the dissipation rate is elevated in the vicinity of the bore (Jinadasa et al., 2016, in this issue). The water on the north (downstream) side of the bore had surface temperature and

salinity that gently decreased northward.

Observing a freely propagating bore in the open ocean, far away from sources of freshwater input, has important implications for the vertical structure of the surface layer and thus the air-sea interactions across the layer. Propagation of the bore creates a barrier layer with a sharply elevated salinity contrast with the water underneath. Barrier layers are ubiquitously found in the Bay of Bengal (Vinaychandran et al., 2002), and it is well known that the presence of a barrier layer plays an important role in the thermal exchange across the ocean surface layer. Furthermore, since the bore is partially temperature-salinity (T-S) compensated (e.g., T increases with S), as the bore brings colder water on top of warmer water, it creates a thermal inversion. Warm water is trapped in the region through which the bore passes. In observations, thermal inversions are often found to accompany barrier layers. Heat trapped in the thermal inversion layer can abruptly change the SST when surface processes erode the barrier layer.

Motivated by the observations and the potential importance of internal bores to the vertical structure of stratification in the ocean surface layer, we use LES to investigate how the lateral density gradient influences the propagation of the bore as well as its mixing properties. The flow physics of the conventional lock exchange problem (Härtel et al., 2000; Cantero et al., 2008) is modified in this problem by adding the effects of the constant horizontal gradient of temperature and salinity in the ambient fluid and the Coriolis force associated with Earth's rotation. The model setup consists of the upper-ocean surface layer at 16.1°N with the salinity and temperature fields similar to those in the 2013 observation. The top 50 m is the surface mixed layer where the temperature decreases at the rate of 3.5×10^{-5} °C m^{-1} and the salinity decreases at the rate of 7.5×10^{-5} psu m^{-1} northward. The left-wall boundary condition corresponds to fresher and cooler water in the top 50 m with a temperature difference of 0.5°C and a salinity difference of 0.6 psu with respect to the interior. This buoyancy contrast (without momentum flux input) drives the gravity current that propagates across the domain.

The left wall has free-slip velocity boundary conditions with the salinity and temperature fixed over the top 50 m. The boundary condition at the left wall is uniform in the along-bore direction. At the right wall, the velocity

Box 1. Multiscale Observations of Near-Surface Salinity in the Bay of Bengal

By Jonathan D. Nash, Andrew J. Lucas, Jennifer A. MacKinnon, Emily L. Shroyer, Caitlin B. Whalen, and Amy F. Waterhouse

High rainfall and freshwater river input into the Bay of Bengal conspire to produce strong vertical and horizontal gradients in near-surface salinity on many different scales. O(1 psu) changes in salinity over a few meters in the vertical are not uncommon; similar gradients can even be observed in the horizontal on some occasions (see below). A unique perspective of these gradients was obtained during ASIRI, where observations of near-surface temperature and salinity were obtained with 2 m horizontal resolution over lateral expanses exceeding 500 km.

Figure B1 shows northern Bay of Bengal salinity sections sampled from R/V *Roger Revelle* at three different scales, using three different types of sampling at three different locations at three different times. At the largest scale (Figure B1a), a 2015 section using Scripps Institution of Oceanography's Fast CTD (conductivity-temperature-depth instrument) at an average spatial resolution of 460 m captures a broad 3 psu change in surface salinity over 150 km, a gradient characteristic of this region. It also shows sharper fronts (between 120 km and 140 km) where the salinity changes by O(1 psu) over O(1–10 km) scales. However, salinity remains relatively constant at 50 m depth, which also produces strong lateral gradients in salinity-induced vertical stratification. The lateral gradient in salinity is not monotonic, such that there are gradients of both signs over this horizontal scale. On a slightly smaller scale (b), measurements made by a profiling RBR CTD in 2013 at an average spatial resolution of 850 m reveal considerable structure in salinity on 1–5 km scales and associated variability in both vertical and lateral gradients (contours are salinity at 0.1 psu intervals); at these scales, the physics are expected to be controlled by processes that unite the vertical and horizontal, and may be signatures of submesoscale instability based on the process modeling discussed in the main text. Freshwater features appear to have scales much smaller than the transect length so that gradients have both signs. At finer scales (Figure B1c), measurements from a towed bow chain with 15 thermistors and four CTDs are used to infer salinity with 2 m horizontal and 0.5 m vertical resolution. While there are times when all sensors yield the same temperature and salinity throughout the upper 10 m, these sections also have times characterized by sharp horizontal gradients within the layer. This feature, observed in November 2013, appears to behave as an internal bore, which at its front had approximately 0.5 psu change in salinity over just a few meters and which propagated at the speed of an internal gravity current. The bore exhibits a strongly undulating tail that is similar to those modeled in this paper and observed in the lab with instabilities on a variety of length scales.

AUTHORS

Jonathan D. Nash and **Emily L. Shroyer** are at the College of Earth, Ocean, and Atmospheric Sciences, Oregon State University, Corvallis, OR, USA. **Andrew J. Lucas**, **Jennifer A. MacKinnon**, **Caitlin B. Whalen**, and **Amy F. Waterhouse** are at Scripps Institution of Oceanography, University of California, San Diego, La Jolla, CA, USA.

boundary condition is free slip and the scalar boundary condition is no flux. The top boundary is also a free-slip, no-flux surface. A sponge region is used in the bottom 20 m of the domain. In the sponge region, velocity is damped toward zero, while salinity and temperature are damped to the background gradients.

The computational domain is 8.2 km in the cross-bore direction, 64 m in the along-bore direction, and 127 m in the vertical direction using a grid of 16,384 × 128 × 256 points, respectively. The horizontal grid resolution is 0.5 m while the vertical grid resolution in the top 50 m is 0.25 m. In the region below 50 m depth, the vertical grid resolution gradually increases to a maximum value of 3 m at 127 m depth. The LES subgrid fluxes are computed using a dynamic Smagorinsky model. Unity subgrid Prandtl and Schmidt numbers are employed to compute subgrid heat and salinity fluxes. The simulation is performed for a time period of eight physical hours using 60,000 computational hours on a 256-processor supercomputer.

Upon the release of the fresher and cooler water, a bore immediately forms as shown in Figure 1. Cooler and fresher water from the south (left) flows over warmer and saltier water in the north (right), creating the bore. As the bore passes, a barrier layer is formed with stratification sharply elevated at 25 m depth. A thermal inversion layer is formed between 25 m and 50 m depth where the water is up to 0.4°C warmer than the SST. The bore is highly nonlinear. Shear instabilities grow along the interface of the bore and develop into Kelvin-Helmholtz (KH) billows. The billows become larger as they advect toward the back of the bore and break down into turbulence. The resulting dissipation rate is intense, with a value in the order of 10^{-6} m^2 s^{-3}.

A zone of surface flow convergence forms ahead of the bore, as shown by the velocity vectors (arrows) in Figure 2. As the bore propagates to the right, the pressure gradient generated by the lateral density gradient in the background drives a leftward countercurrent opposing the bore. This creates a zone in front of the bore with strong downward flow. The downward flow, unable to penetrate the pycnocline, splits into two currents that flow horizontally away from the bore in the bottom half of the surface layer. Some of the water from the ambient flow returns toward the right of the domain while some subducts below the bore and travels toward the left of the domain. The

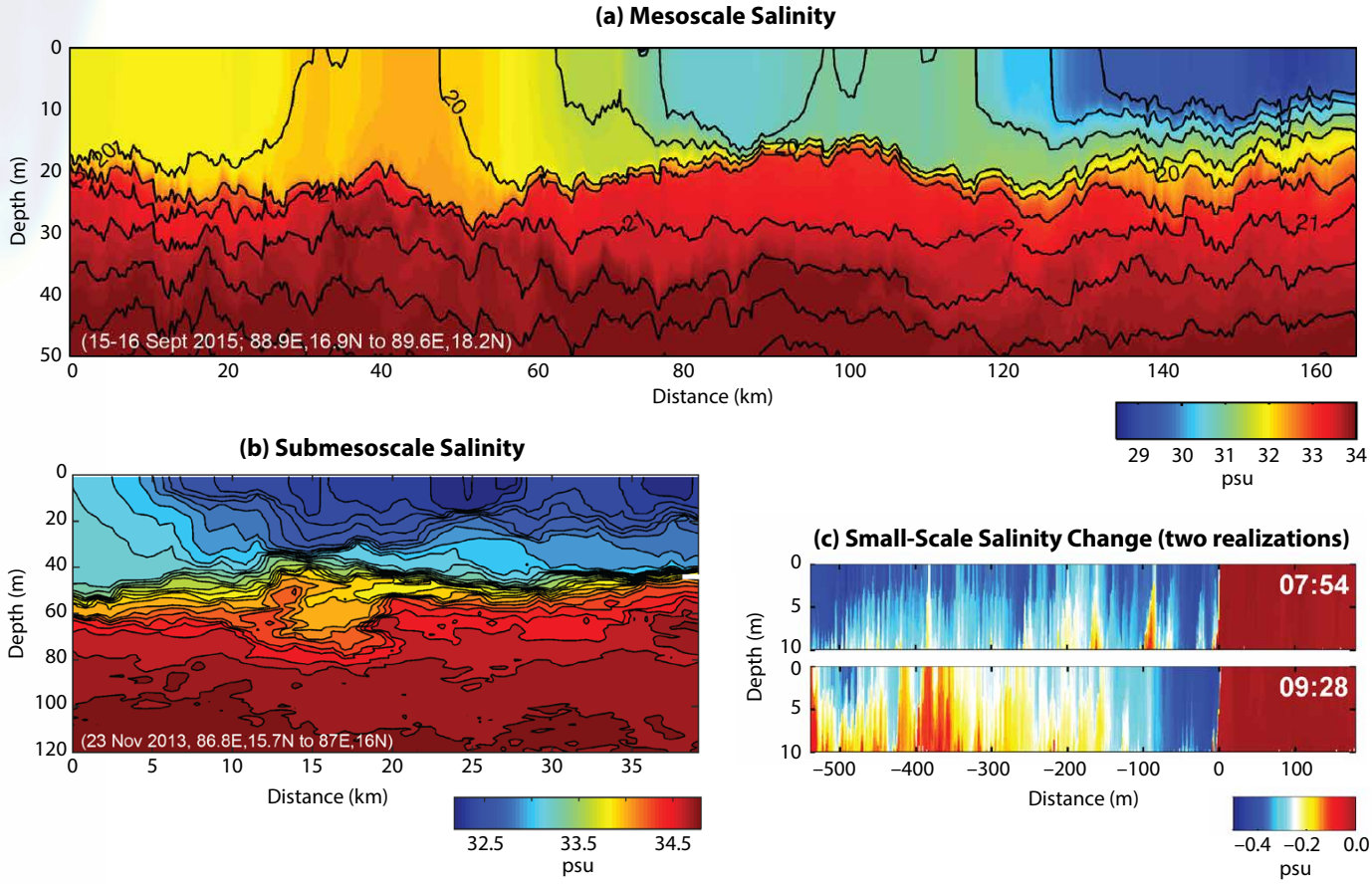

FIGURE B1. Salinity sections collected from R/V *Roger Revelle* in the northern Bay of Bengal are shown at three different scales, using three different types of sampling at three different locations at three different times. See box text for figure details.

resulting currents create strong vertical shear, both behind and ahead of the bore.

The bore in the simulation rotates owing to the Coriolis effect and decelerates as it propagates, features that are also shared by the bore observed in Figure B1c. We find the lateral density gradient influences the speed in two ways. First, the density jump and, therefore, the pressure gradient driving the bore decrease as the bore propagates. The smaller the density jump, the smaller is the driving pressure gradient and thus the smaller is the bore speed. Second, the lateral density gradient also drives a countercurrent in the region ahead of the bore. As the countercurrent gets stronger, the speed of the bore decreases until it is arrested at approximately 3 km.

By using a high-resolution LES model, we can construct a model bore with features similar to the observed bore in the Bay of Bengal. With such agreement, the model complements the observational data by providing a validated tool to describe the evolution of the bore at high temporal and spatial resolution. This is important for quantifying local mixing of the complex horizontal and vertical gradients of salinity and temperature that develop in the Bay of Bengal.

INSTABILITY AND TURBULENCE AT STRONG FRONTAL ZONES

The data collected during the ASIRI cruises in the northern BoB (Figure B1b, for example) feature continuous lateral variation of salinity along the ship track. The strength of the lateral density gradient $M^2 = -g/\rho_0 \, d\rho/dy$ is found to vary over a wide range of values. It is believed that the lateral density gradient is associated with frontal instabilities that mediate the forward energy cascade from mesoscale eddies to small-scale turbulence and dissipation. Many different types of instability such as baroclinic instability, mixed layer instability, and symmetric instability are possible (Thomas et al., 2013), with correspondingly different routes to turbulence. M^2/f^2 is a convenient nondimensional measure of the horizontal gradient of buoyancy, and the value of M^2/f^2 can be as large as 800 while the typical range is between 50 and 200. The connection of submesoscale instabilities and turbulence to observations of salinity variation over a wide range of horizontal and vertical scales (Figure B1) is not clear.

Motivated by the open questions

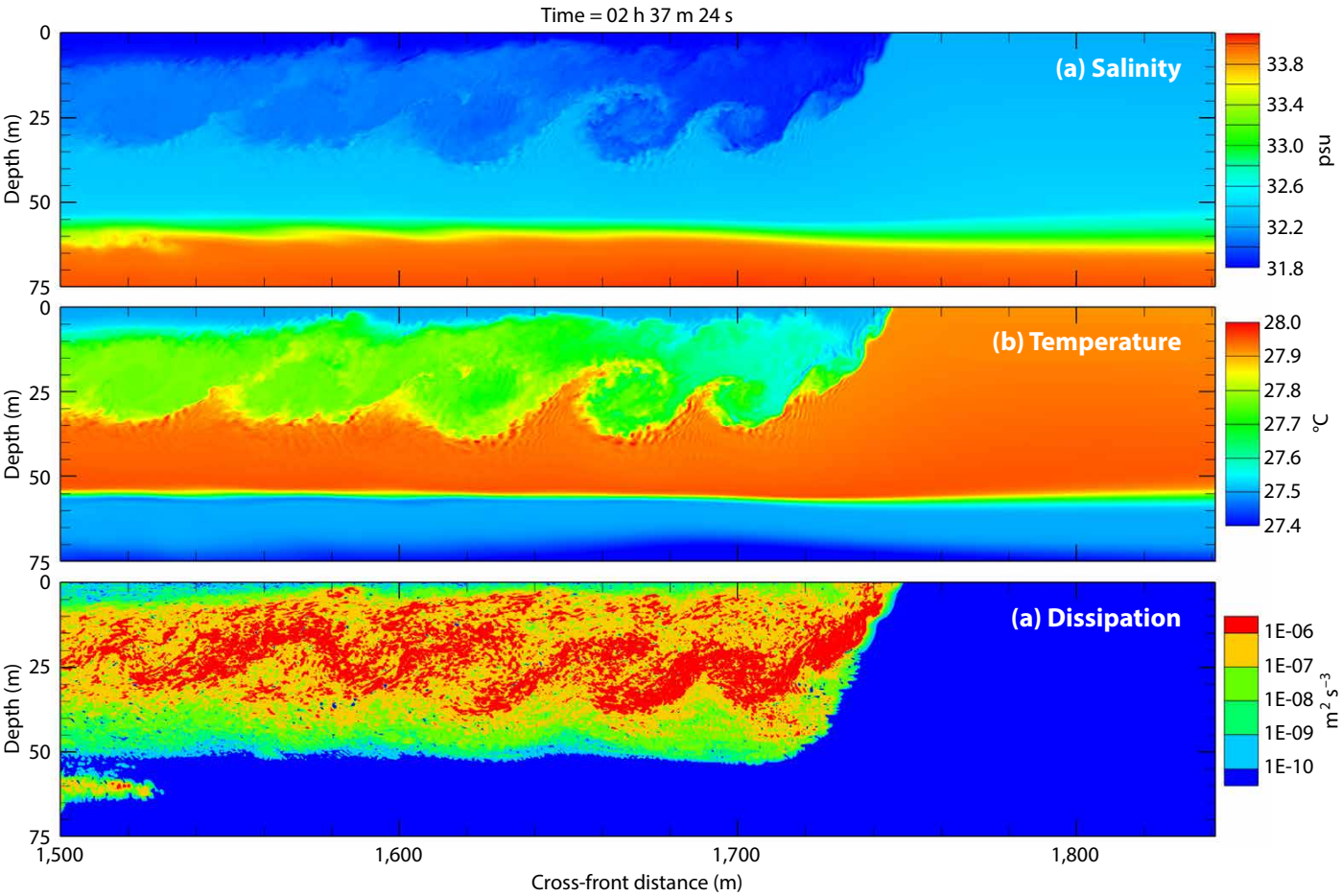

FIGURE 1. Structure of the bore in the large eddy simulation (LES). As the bore propagates across the ocean surface layer from left to right, colder and fresher water from the left side of the domain flows on top of warmer and saltier ambient water. As the bore passes, a barrier layer is formed with sharply elevated stratification at 25 m depth and a thermal inversion layer between 25 m and 50 m depth. Kelvin-Helmholtz shear instability develops at the interface between the bore and the ambient water. The resulting turbulence generates intensive mixing with a dissipation rate elevated up to 10^{-6} m^{-2} s^{-3}.

about turbulence and stratification structure associated with frontal instabilities, we examine the evolution of a frontal zone with a large horizontal buoyancy gradient using LES. We model a frontal region in the ocean surface layer that is uniformly stratified in both the horizontal and vertical directions with uniform M^2 and N^2, respectively. The front is balanced by a geostrophic current U(z) such that the shear rate $S = dU/dz = -M^2/f$. The current is shear-stable with the gradient Richardson number $Ri_g = N^2/S^2 = 0.5$ such that shear instability is unable to develop. However, the flow is subject to the so-called symmetric instability, which is known to develop for the range of $0.25 < Ri_g < 1$ (Thomas et al., 2013). Because this instability has perturbations that are symmetric (i.e., no variation, in the along-front direction), we use the term "symmetric instability" to describe this feature.

The computational domain is 4.1 km in the cross-front direction, 256 m in the along-front direction, and 96 m in the vertical direction using a grid of 2,048 × 128 × 96 points, respectively. The domain has 2 m grid resolution in the horizontal directions and 1 m resolution in the vertical direction. The LES subgrid fluxes are computed following the model introduced by Ducros et al. (1996). The simulation is performed over a wall-clock time of 20 days on a 256-processor supercomputer.

Since only a few previous studies focus on the turbulence aspects of this moderate-Ri_g instability (Taylor and Ferrari, 2009, 2010; Arobone and Sarkar, 2015), current knowledge of the process is limited. Our objective is to further explore the turbulent processes that can possibly equilibrate fronts. Our simulations portray a process starting with the growth of symmetric instability, followed by the development of secondary KH shear instability and subsequent turbulent mixing. When the symmetric instability develops, bands of positive and negative cross-front velocity grow into finite amplitude leading to an increase in vertical shear. The vertical shear becomes unstable to KH shear instability and develops billows. Finally, the billows break down into turbulence and mix fluid across isopycnals. Note that as we increase the along-front domain, the mode that emerges and breaks down into turbulence is not symmetric. The bands of positive and negative cross-front velocity exhibit variations in the along-front direction owing to a horizontal tilt at angle of ~4° with respect to the along-front direction from the heavier side of the front toward the lighter side. Jones and Thorpe (1992) explored the emergence in nonhydrostatic simulations of an asymmetric mode that developed during transient growth in the Eady problem by Salhi and Pieri (2014), and it was shown to be involved in the ultimate breakdown to turbulence in the simulations of Arobone and Sarkar (2015).

Interestingly, the process does not occur throughout the cross-front direction but rather in localized patches, as shown in Figure 3. The patches result from secondary KH shear instability, with billows that mix along the slanted isopycnals and destroy the lateral gradients. At the same time, isopycnals are compressed into frontal bands. The bands with compressed isopycnals have

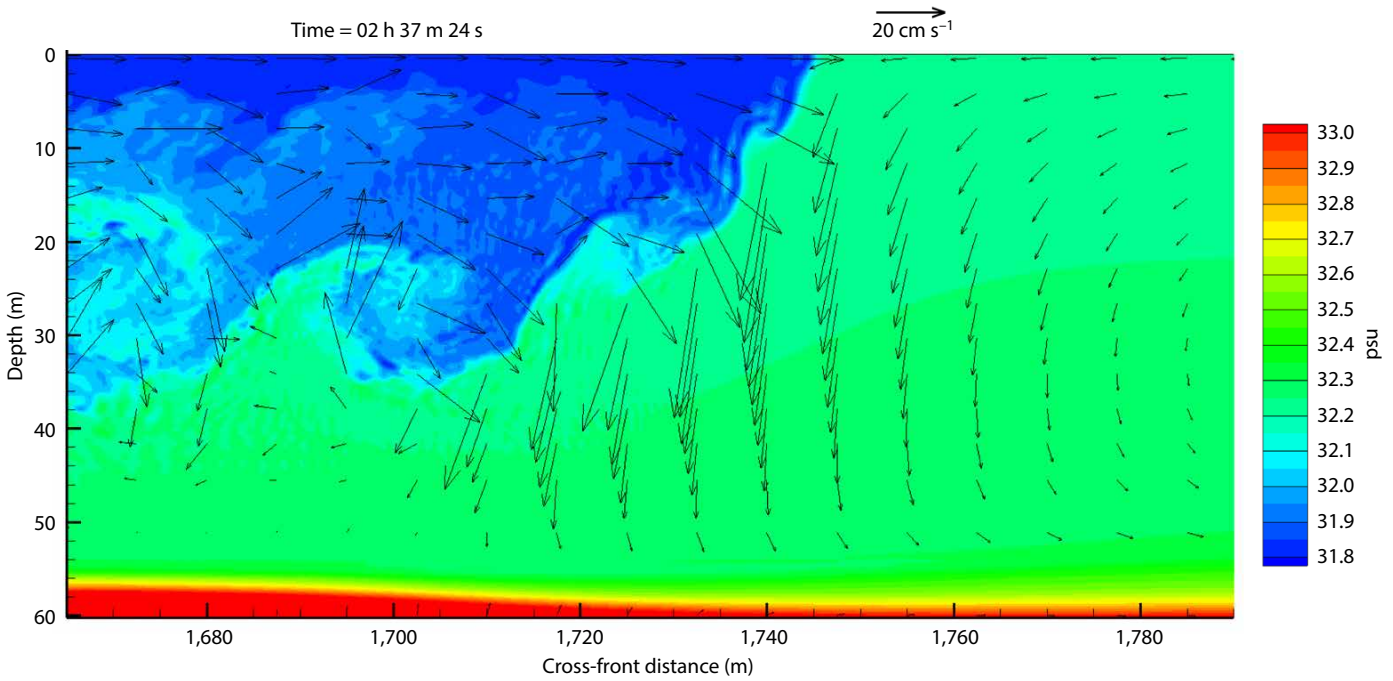

FIGURE 2. Velocity field (vectors) and salinity field (color contours) at the head of the bore in the LES. The bore brings fresher water from the left to the right. It is opposed by a countercurrent that is driven by the favorable pressure gradient associated with the ambient lateral density gradient. The two currents converge ahead of the bore and drive a strong downward flow. Some of the saltier ambient water subducts down into the region below the bore.

stronger density gradients, in both lateral and vertical directions, and also stronger vertical shear. Subsequently, the bands with compressed isopycnals undergo KH shear instability and are broken down into thinner bands.

The turbulent process illustrated in Figure 3 suggests a possible route in which a strong, large-scale horizontal gradient is broken down into thinner but sharper fronts (bands of compressed isopycnals) through turbulent processes. Turbulence in the surface layer is layered in both horizontal and vertical directions and remains persistent over many inertial periods. It is interesting that the magnitude of M^2/f^2, initially equal to 50 through the cross-front direction, can increase to a significantly larger value in localized bands of compressed isopycnals. The disintegration of a large frontal zone into smaller frontal bands through symmetric instability seen in the simulation is one possible explanation for the numerous sharp narrow fronts at scale of a few kilometers seen in the observations.

The instabilities seen in the present simulations are highly three dimensional and range in scale from a few meters to hundreds of meters in the horizontal and a few meters in the vertical (Figure 4). In the top-down view of the front at 25 m depth, we see density intrusions that are tilted at an angle of approximately 45° to the along-front direction and have a horizontal scale of ~50 m. In the cross-front view, the KH shear instability develops into billows with overturns at scales of ~10 m, similar to the 10 m overturn scale evident in Figure B1c. These overturns mix fluid starting from near the surface at the heavier side, moving along the isopycnals toward the bottom of the surface layer at the lighter side. Multiple downward-moving overturns can occur at the same time so that a vertical profile would show turbulence in multiple layers across the top 50 m. In the along-front view, shear instability also develops with a horizontal scale of ~100 m, and it can develop billows with a vertical scale of ~10 m. The present simulation illustrates that the processes through which a front slumps and equilibrates can be dynamically rich with small-scale ageostrophic features and turbulent mixing.

Through the disintegration of the front, the potential energy available in the lateral density gradient is released for turbulence and mixing. The surface layer becomes more stratified; the squared buoyancy frequency N^2 at a late stage is approximately twice as large with respect to the value at the initial state. The increase in N^2 is not vertically uniform. There are multiple layers with

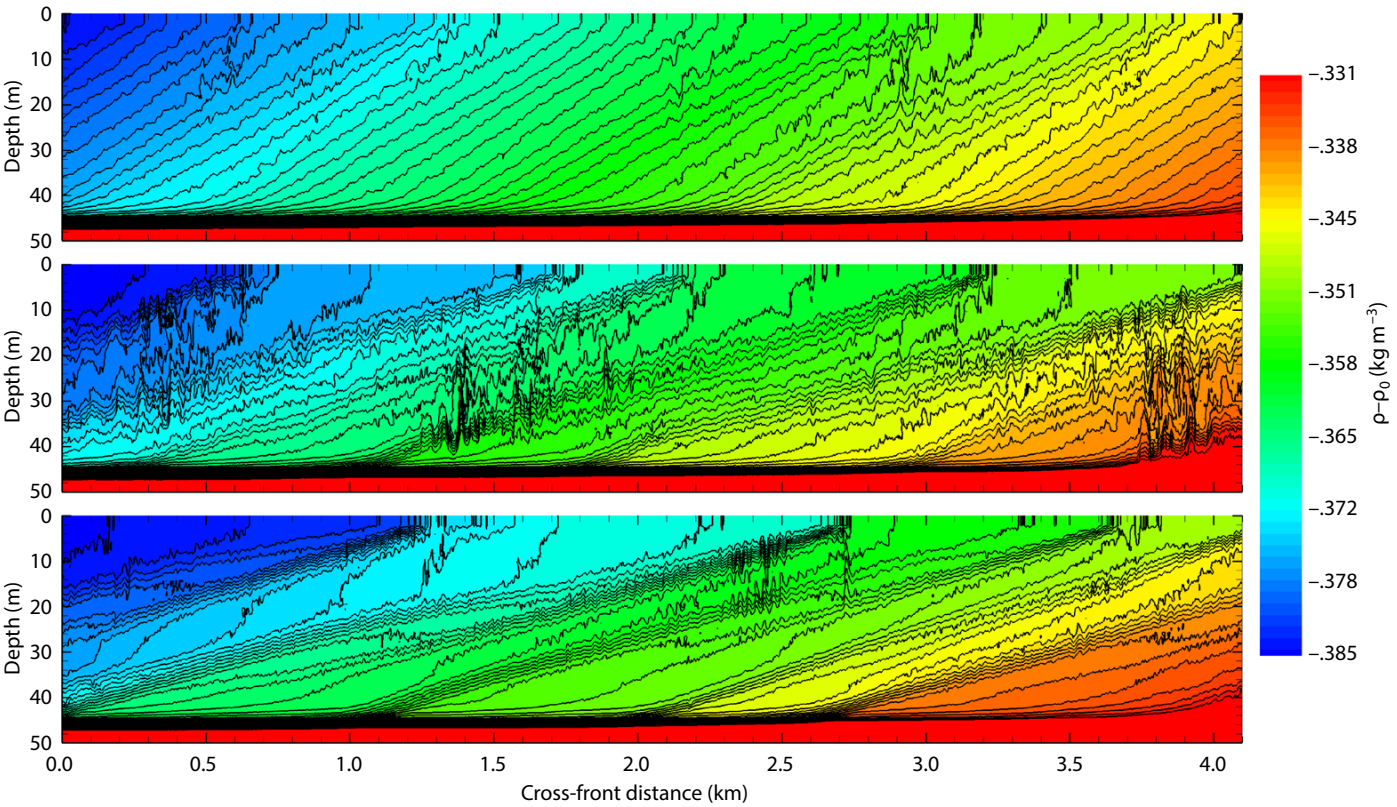

FIGURE 3. Snapshots of the density deviation (from a reference value) shows generation of frontal turbulence at different times during the simulation with $M^2/f^2 = -50$. Initially, the front has constant lateral and vertical density gradients and is in geostrophic balance. (a) Symmetric instability develops with bands of positive and negative cross-front velocity along the isopycnals. The cross-front velocity increases vertical shear and leads to Kelvin-Helmholtz shear instability. (b) The Kelvin-Helmholtz billows mix waters of different density in localized patches and create bands of compressed isopycnals. The bands have elevated shear and lateral and vertical density gradients. (c) The bands undergo subsequent Kelvin-Helmholtz shear instability and further erode the lateral gradient.

enhanced N^2 sandwiched between layers with smaller values of N^2. The vertical shear rate also shows layering features. The gradient Richardson number in the surface layer gradually increases over time and reaches unity near the end of the simulation. The instability of slantwise currents persists for a long time, and it oscillates at the inertial frequency.

RESPONSE OF A SUBMESOSCALE FRONT TO WIND AND THERMAL FORCING

One of the challenges in the BoB is to understand how processes across a range of scales interact within the shallow surface layer. In this section, we focus on the submesoscales to seek dynamical links between frontal processes occurring at O(1–10 km) scales and the vertical structure of the upper BoB during the southwest monsoon (Figure B1a). We use idealized three-dimensional simulations to identify potential mechanisms responsible for anomalously low stratification at intermediate depths, one of the defining features of the upper bay during the monsoon season.

Model Setup

For these three-dimensional simulations, we use the Process Study Ocean Model (PSOM) (Mahadevan, 2006). PSOM is a three-dimensional, nonhydrostatic, Boussinesq model where the top layer of grid cells follows the free surface. The model allows for topography, although the simulations in this study use a flat bottom boundary. The zonal and meridional extent of the simulated domain is 288 km and 576 km, respectively. The horizontal grid resolution in both directions is 1 km. The depth of the domain is 400 m. The model uses a stretched vertical grid of O(1m) resolution in the top few meters and O(10m) resolution in the bottom layers of the domain. We have coupled PSOM to the General Ocean Turbulence Model (GOTM), developed by Burchard et al. (1999), such that the prognostic equations used to evolve the model variables in PSOM use the vertical eddy viscosities obtained from one of the many turbulent parameterizations in GOTM (Mukherjee et al., 2012). For vertical mixing we use k-ε, a two-equation turbulence parameterization (Canuto et al., 2001) that evolves in time the subgrid-scale kinetic energy (k) and the subgrid dissipation (ε). In our implementation, k and ε are not advected by the resolved-scale velocity fields. We parameterize horizontal subgrid mixing using a constant subgrid viscosity of 0.1 $m^2 s^{-1}$. For the optical properties, we use extinction coefficients for the surface waters of the BoB (Lotliker et al., 2016, in this issue).

The simulations are initialized with temperature and salinity data obtained from a pair of Argo floats in the northern Bay of Bengal (near 18°N) during August 2013 to set up an initial meridional gradient in density typical of the northern bay during the southwest monsoon. Near the surface, the lighter, fresher waters are to the north, while the heavier, saltier waters are to the south. The surface front describes a variation in density of 2 kg m^{-3} over 15 km, which corresponds to a buoyancy gradient of 1.5×10^{-6} s^{-2}. Such strong gradients over O(10 km) scales, observed during the August 2015 cruise, are an order of magnitude larger than those considered in most earlier studies of open-ocean frontal systems (see Introduction). Below 20 m, there is a reversal of the meridional

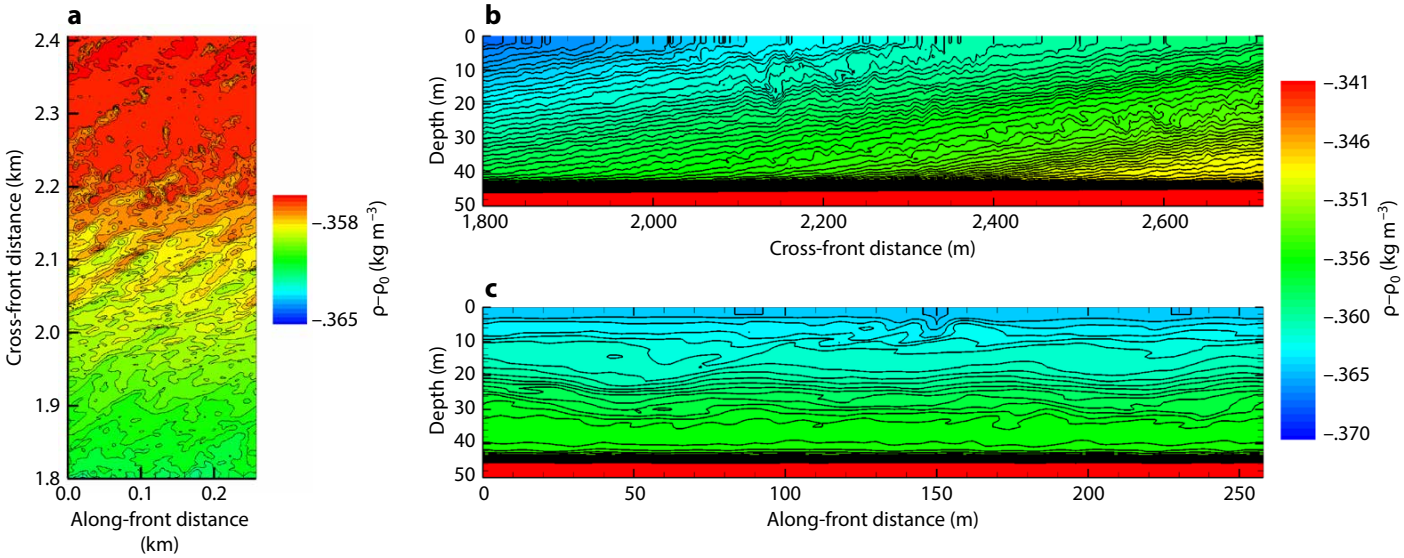

FIGURE 4. A three-dimensional structure at small scale is illustrated using the density deviation (from a reference value) in the simulation with $M^2/f^2 = -50$. (a) A top-down view at 25 m depth shows fluids intruding from the lighter side toward the heavier side of the front at about 45°. The intrusions have a horizontal scale of ~50 m. (b) A cross-front view shows the development of Kelvin-Helmholtz billows along the isopycnals. The Kelvin-Helmholtz billows form in multiple bands with vertical scale of ~10 m. (c) An along-front view shows shear instabilities with horizontal wavelength of ~100 m and isopycnal overturns with vertical scale of ~10 m. The localized turbulent mixing creates layers of different stratification across the surface layer.

buoyancy gradient whose magnitude then decreases gradually to zero at a depth of 100 m, below which all models fields are horizontally uniform at the start of the simulation. We prescribe the initial velocity fields to be in thermal-wind balance with the front.

We force the three-dimensional model with hourly momentum and thermal fluxes derived from the 18°N Woods Hole Oceanographic Institution mooring (Weller et al., 2016, in this issue) for the period August 15–26, 2015. To avoid impulsive forcing, the fluxes ramp up linearly from zero to their initial values (on August 15) over one inertial period. The winds are predominantly from the southwest during this period, as is typical during the summer monsoon. The simulations have no precipitation.

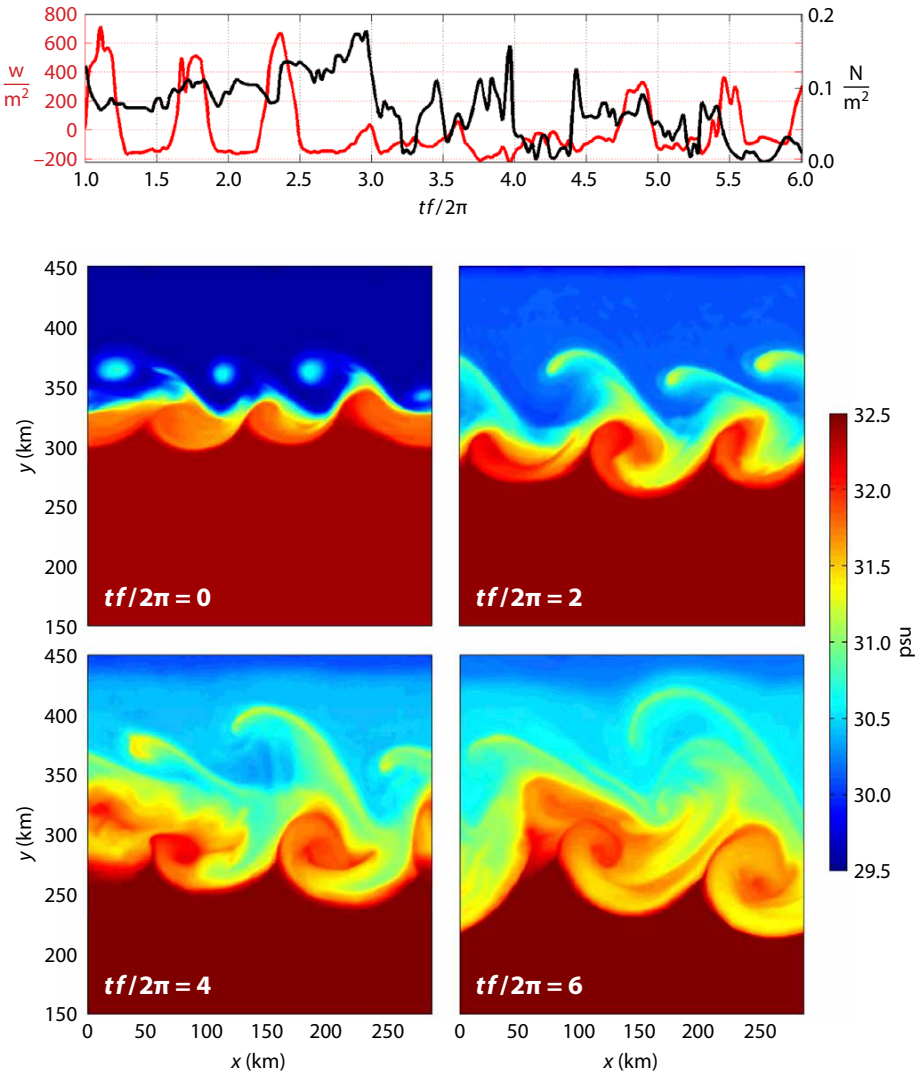

FIGURE 5. (top) The winds and net thermal fluxes used to force the model. At 18°N, one inertial period is approximately equal to 39 hours. (bottom) Evolution of salinity at 2 m depth. The nondimensional time shown above each image marks the time elapsed since the surface forcing is turned on (t = 0), after the front has gone unstable (2), when mixed-layer instabilities begin to form (4) (Boccaletti et al., 2007; Fox-Kemper et al., 2008), and when eddies started to form (6). Until this time (eight inertial periods), the front evolves without any surface forcing. In the presence of winds and thermal air-sea fluxes, the meanders continue to grow, generating salty filaments with O(f) relative vorticities (plot not shown). The wind direction is predominantly from the southwest during the summer monsoon, which corresponds to an upfront orientation for the large-scale meridional density gradient in the Bay of Bengal. The southward propagation of the front over time is consistent with the expected Ekman transport for a southwesterly wind.

We use PSOM in a channel configuration, with periodicity in the zonal direction and rigid walls at the meridional boundaries (Mahadevan, 2006). We evolve the initial condition for eight inertial periods by which time the front has gone unstable, creating mixed layer instabilities (Tandon and Mahadevan, 2006; Boccaletti et al., 2007) and developing eddies (Figure 5). At this point, the winds and thermal air-sea fluxes are turned on. The southwesterly winds yield an "upfront" orientation for the large-scale meridional density gradient in the BoB, implying advection of lighter fluid over heavier fluid by Ekman currents. At smaller scales, both upfront and downfront winds are a possibility, depending on the alignment of the frontal meanders with the wind. For the rest of our analysis, we measure time from the moment the fluxes are turned on.

Near the surface (2 m depth; Figure 5), stirring by eddies creates dense, salty filaments O(100 km) long. Relative vorticity, ζ, at the edge of these filaments is O(f) (plot not shown), reflecting an O(1) Rossby number, typical of circulations associated with instabilities of mixed layer fronts (Tandon and Mahadevan, 2006; Capet et al., 2008). The mean location of the front shifts southward over time, qualitatively consistent with the expected Ekman transport for a southwesterly wind. As the fresh waters advect southward, they also become saltier due to vertical mixing events, parameterized here through the two-equation model.

One of the prominent features in our simulations is the widespread occurrence of weakly stratified regions at intermediate depths (Figure 6). This is also one of the striking features of the upper BoB during the southwest monsoons that are often seen in observations, including the recent measurements that are the focus of this special issue (Figure B1). The weakly stratified regions are characterized by: (1) anomalously low Ertel potential vorticity, PV = $\omega_a \nabla b$, where ω_a

is the absolute vorticity vector and b is the buoyancy; (2) anticyclonic relative vorticity; and (3) nonzero stratification and meridional buoyancy gradient. Hence, these regions bear the signatures of intrathermocline eddies, sometimes referred to as submesoscale coherent vortices (SCV) (McWilliams, 1985; Thomas, 2008). In our simulations, the low-PV patches tend to form beneath outcropping fronts by subduction of water masses from near the surface. The subduction occurs near locations associated with convergence in the surface velocity field. The zones of convergence exhibit O(f) cyclonic relative vorticity, consistent with the frontogenesis mechanism described by Hoskins and Bretherton (1972) and documented in past submesoscale-permitting simulations of upper-ocean fronts, although with deeper mixed layers (Tandon and Mahadevan, 2006). A zonal (west-east) section reveals a profusion of low-PV patches along the front (Figure 7). From the two sections (Figures 6 and 7), we infer that the patches are intermittent in space, 10–20 km wide in both zonal and meridional directions, and O(10 m) thick. The weak stratification in the low-PV patches is not a consequence of diapycnal mixing (plot not shown), which is negligible below the top 10–20 m. Rather, the vertical structure in Figures 6 and 7 results from adiabatic subduction near fronts (Pollard and Regier, 1992; Spall, 1995). Once the low-PV patches are formed, they are "capped" by stratified layers (Figure 7) that result from the advection of lighter over heavier fluid due to the upfront orientation of the winds. As the patches can extend up to depths of 40–50 m, the sequence of frontal subduction of anomalous water masses and their subsequent capping has the potential to alter the water-mass properties in the permanent pycnocline.

The three-dimensional simulations hardly exhibit any temperature inversions. Some preliminary studies suggest it is easier to form comparable temperature inversions in the three-dimensional simulations with a surface flux of freshwater. We will be exploring the results from these simulations in greater detail in a future study.

CONCLUDING REMARKS

The surface-layer salinity field in the northern Bay of Bengal is multiscale. A salinity change of 0.5 psu can occur over a horizontal distance of a few kilometers or a horizontal distance of just a few meters. Numerical process studies of different types reported here reveal the rich dynamics that are associated with stirring and mixing of horizontal salinity gradients in the surface layer by submesoscale flow instabilities and turbulence.

A particularly intriguing feature in the observations is the presence of interspersed vertical layers with differing salinity levels in the surface layer. The simulations of a mesoscale domain show that Ekman currents associated with upfront winds and mixed layer instability interact, leading to subduction of low-stratification water masses at fronts. Patches of anomalously low buoyancy and potential vorticity are created with a vertical extent of O(10 m) and horizontal extent of a few kilometers. Turbulence-resolving LES of a stronger front shows

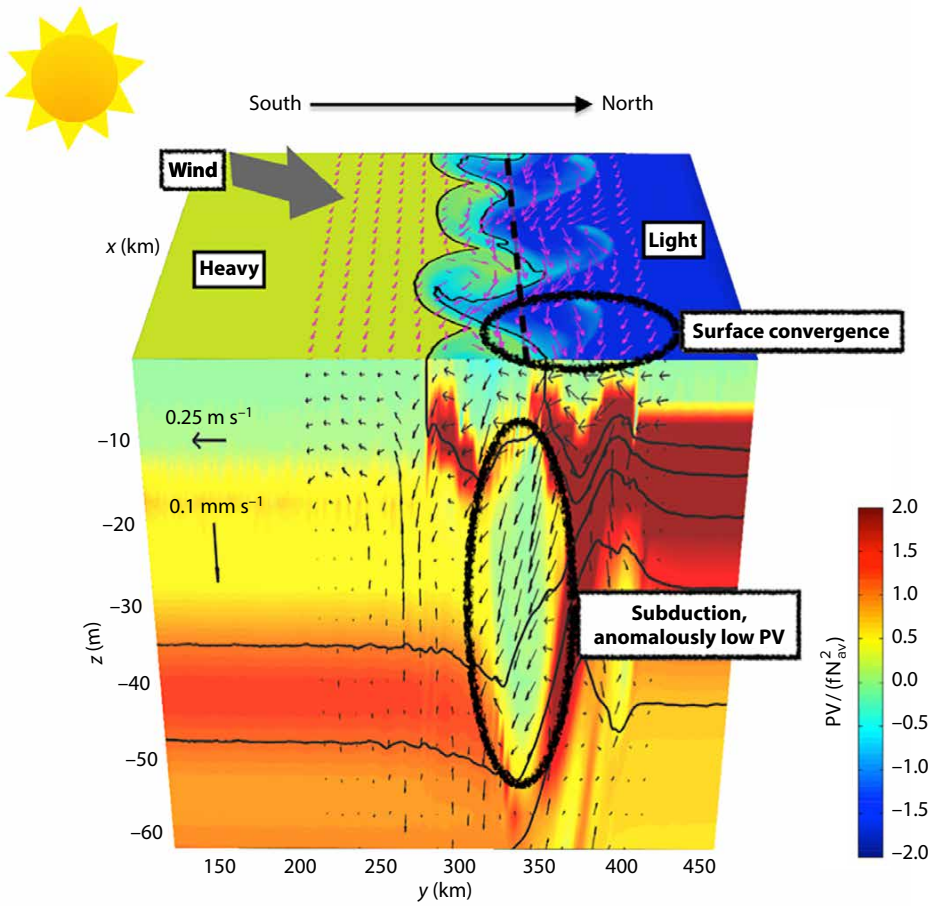

FIGURE 6. Subduction of low nondimensional Ertel potential vorticity (PV) water at fronts generates anomalously low stratification at intermediate depths (Spall, 1995; Thomas, 2008). The top face shows the surface potential density field (color) and horizontal velocity vectors (pink). The fluid is lighter toward the north near the surface, with a reversal of the meridional buoyancy gradient deeper down. The solid lines are isopycnals contoured at intervals of 0.5 kg m^{-3}. The black dashed line on the top face shows the meridional location of zonal (west-east) sections in Figure 7. The vertical face shows a meridional (south-north) section of PV two inertial periods after the forcing has been turned on. The PV has been scaled with fN^2_{av}, where N^2_{av} is the stratification averaged over the vertical section shown in the figure. The gray arrow on the top face indicates the typical wind direction during the simulation. Regions of weak stratification occur at intermediate depths (15–50 m) below surface fronts. These regions are associated with anticyclonic vorticities (see Figure 7) and are formed through subduction of water masses by ageostrophic circulations near fronts. This pattern occurs repeatedly at several locations during the course of the simulation. The meridional extent of these regions is typically O(10 km).

that slantwise currents of symmetric instability and local turbulent mixing by secondary shear instability combine, leading to multiple layers of stratification with a vertical extent of O(10 m) and horizontal extent of O(50 m). Thus, both an adiabatic process and a turbulent process can stir and mix horizontal buoyancy gradients to create vertical buoyancy contrasts, albeit with different horizontal scales.

Nonlinear bores associated with small-scale horizontal gradients at the meter scale have also been observed during the ASIRI cruises. We demonstrate that, with high-resolution LES, it is possible to numerically model the evolution of a nonlinear bore so as to represent the influence of rotation and background stratification on its propagation as well as its influence on turbulence and the buoyancy structure of the surface layer.

Large-scale ocean models resolve horizontal motions with as much resolution as computational resources permit while intensively relying on parameterizations for vertical motions. The instabilities and small-scale features seen in the present study suggest that the dynamically rich processes at fronts pose challenges for parameterizations. The processes at horizontal scales of less than a kilometer are inherently coupled in both horizontal and vertical directions. It is a challenge for next-generation ocean models to include the effects of such multiscale turbulent processes for realistic representation of frontal dynamics, restratification, and air-sea fluxes. Adaptive meshing and nested-grid approaches with embedded LES provide multiscale-resolution capability and will help address the modeling challenge.

REFERENCES

Arobone, E., and S. Sarkar. 2015. Effects of three-dimensionality on instability and turbulence in a frontal zone. *Journal of Fluid Mechanics* 784:252–273, http://dx.doi.org/10.1017/jfm.2015.564.

Boccaletti, G., R. Ferrari, and B. Fox-Kemper. 2007. Mixed layer instabilities and restratification. *Journal of Physical Oceanography* 37:2,228–2,250, http://dx.doi.org/10.1175/JPO3101.1.

Burchard, H., K. Bolding, and M.R. Villarreal. 1999. GOTM–A general ocean turbulence model: Theory, applications and test cases. Technical Report EUR 18745 EN, European Commission.

Cantero, M.I., S. Balachandar, M.H. Garcia, and D. Block. 2008. Turbulent structures in planar gravity currents and their influence on the flow dynamics. *Journal of Geophysical Research* 113, C08018, http://dx.doi.org/10.1029/2007JC004645.

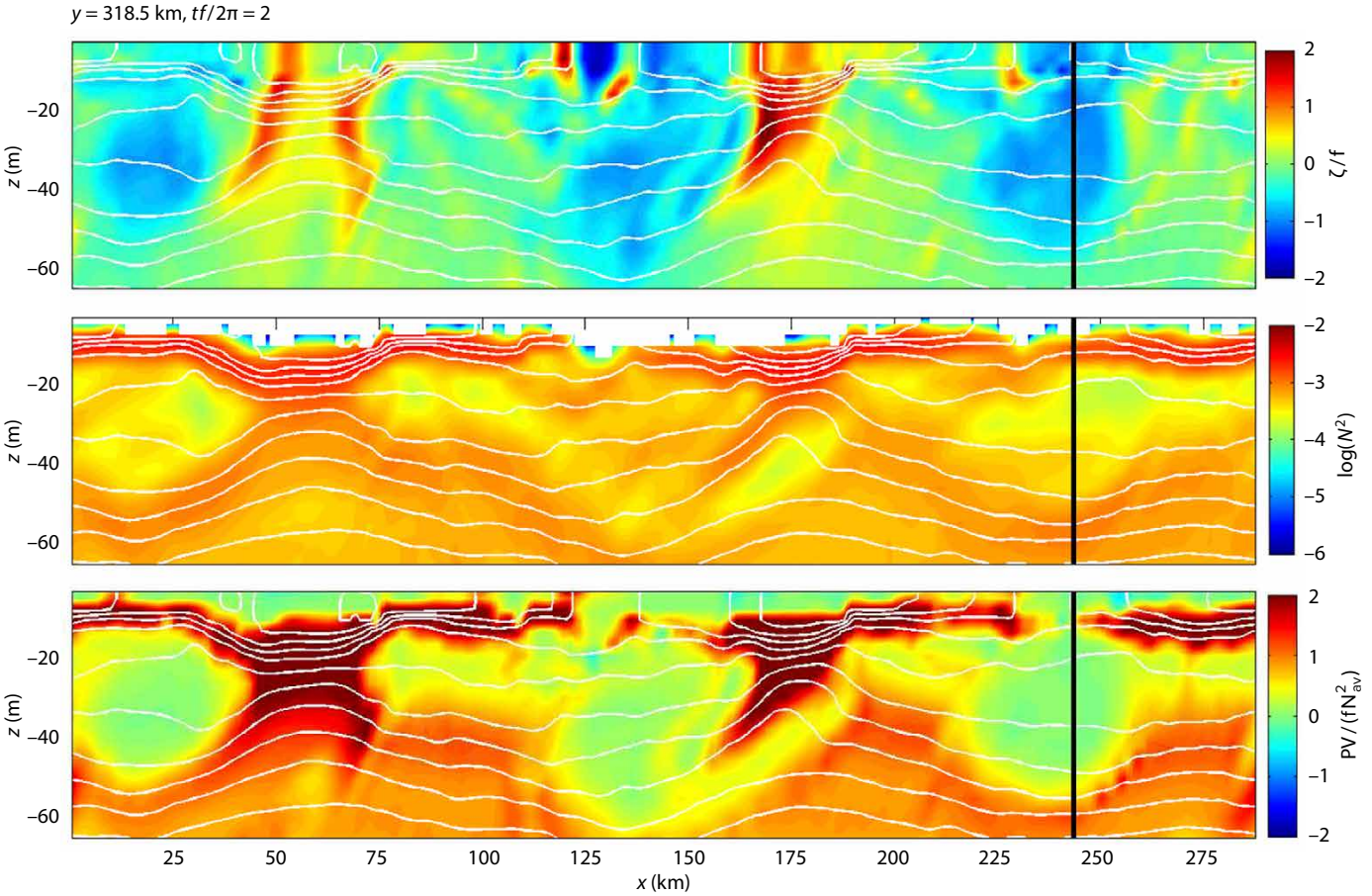

FIGURE 7. Zonal (west-east) sections at two inertial periods after the forcing has been turned on. The fields are (top to bottom): (1) relative vorticity scaled with the Coriolis parameter, (2) log(N^2), and (3) Ertel potential vorticity scaled with fN^2_{av}, where N^2_{av} is the stratification averaged over the area shown in the figure. The white lines are isopycnals contoured at 0.5 kg m^{-3}. The black vertical line shows the zonal location of the meridional section in the previous figure. The section shows several regions characterized by weak stratification, anticyclonic vorticity, and anomalously low PV. After their formation, the low-PV patches tend to get capped by strongly stratified layers due to advection of lighter over heavier fluid, a consequence of upfront winds. Figures 6 and 7 together convey how adiabatic, frontal processes at submesoscales can generate weakly stratified regions at intermediate depths in the upper Bay of Bengal during monsoon conditions.

Canuto, V.M., A. Howard, Y. Cheng, and M.S. Dubovikov. 2001. Ocean turbulence: Part I. One-point closure model—momentum and heat vertical diffusivities. *Journal of Physical Oceanography* 31(6):1,413–1,426, http://dx.doi.org/10.1175/1520-0485(2001)031<1413:OTPIOP>2.0.CO;2.

Capet, X., J.C. McWilliams, M.J. Molemaker, and A.F. Shchepetkin. 2008. Mesoscale to submesoscale transition in the California Current System: Part I. Flow structure, eddy flux, and observational tests. *Journal of Physical Oceanography* 38(1):29–43, http://dx.doi.org/10.1175/2007JPO3671.1.

Ducros, F., P. Comte, and M. Lesieur. 1996. Large-eddy simulation of transition to turbulence in a boundary layer developing spatially over a flat plate. *Journal of Fluid Mechanics* 326:1–36, http://dx.doi.org/10.1017/S0022112096008221.

Fox-Kemper, B., R. Ferrari, and R.W. Hallberg. 2008. Parameterization of mixed layer eddies: Part I. Theory and diagnosis. *Journal of Physical Oceanography* 38:1,145–1,165, http://dx.doi.org/10.1175/2007JPO3792.1.

Gordon, A.L., E.L. Shroyer, A. Mahadevan, D. Sengupta, and M. Freilich. 2016. Bay of Bengal: 2013 northeast monsoon upper-ocean circulation. *Oceanography* 29(2):82–91, http://dx.doi.org/10.5670/oceanog.2016.41.

Härtel, C., E. Meiburg, and F. Necker. 2000. Analysis and direct numerical simulation of the flow at a gravity current head: Part I. Flow topology and front speed for slip and no-slip boundaries. *Journal of Fluid Mechanics* 418:189–212, http://dx.doi.org/10.1017/S0022112000001221.

Hoskins, B.J., and F.P. Bretherton. 1972. Atmospheric frontogenesis models: Mathematical formulation and solution. *Journal of Atmospheric Sciences* 29(1):11–37, http://dx.doi.org/10.1175/1520-0469(1972)029<0011:AFMMFA>2.0.CO;2.

Jinadasa, S.U.P., I. Lozovatsky, J. Planella-Morató, J.D. Nash, J.A. MacKinnon, A.J. Lucas, H.W. Wijesekera, and H.J.S. Fernando. 2016. Ocean turbulence and mixing around Sri Lanka and in adjacent waters of the northern Bay of Bengal. *Oceanography* 29(2):170–179, http://dx.doi.org/10.5670/oceanog.2016.49.

Jones, S., and A. Thorpe. 1992. The three-dimensional nature of 'symmetric' instability. *Quarterly Journal of the Royal Meteorological Society* 118:227–258, http://dx.doi.org/10.1002/qj.49711850404.

Lotliker, A.A., M.M. Omand, A.J. Lucas, S.R. Laney, A. Mahadevan, and M. Ravichandran. 2016. Penetrative radiative flux in the Bay of Bengal. *Oceanography* 29(2):214–221, http://dx.doi.org/10.5670/oceanog.2016.53.

Mahadevan, A. 2006. Modeling vertical motion at ocean fronts: Are nonhydrostatic effects relevant at submesoscales? *Ocean Modelling* 14:222–240, http://dx.doi.org/10.1016/j.ocemod.2006.05.005.

McWilliams, J.C. 1985. Submesoscale, coherent vortices in the ocean. *Reviews of Geophysics* 23(2):165–182, http://dx.doi.org/10.1029/RG023i002p00165.

Mukherjee, S., A. Tandon, and A. Mahadevan. 2012. Submesoscale process studies using a new variant of second order closure. Poster presented at American Geophysical Union Fall Meeting, December 3–7, 2012, San Francisco, CA.

Pollard, R.T., and L.A. Regier. 1992. Vorticity and vertical circulation at an ocean front. *Journal of Physical Oceanography* 22(6):609–625, http://dx.doi.org/10.1175/1520-0485(1992)022<0609:VAVCAA>2.0.CO;2.

Salhi, A., and A.B. Pieri. 2014. Wave-vortex mode coupling in neutrally stable baroclinic flows. *Physical Review E* 90:1–15, http://dx.doi.org/10.1103/PhysRevE.90.043003.

Shcherbina, A.Y., M.A. Sundermeyer, E. Kunze, E. D'Asaro, G. Badin, D. Birch, A.-M.E.G. Brunner-Suzuki, J. Calles, B.T. Kuebel Cerventes, M. Claret, and others. 2015. The LatMix summer campaign: Submesoscale stirring in the upper ocean. *Bulletin of the American Meteorological Society* 96:1,257–1,279, http://dx.doi.org/10.1175/BAMS-D-14-00015.1.

Spall, M. 1995. Frontogenesis, subduction and cross-front exchange at upper ocean fronts. *Journal of Geophysical Research* 100(C2):2,543–2,557, http://dx.doi.org/10.1029/94JC02860.

Tandon, A., and A. Mahadevan. 2006. An analysis of mechanisms for submesoscale vertical motion at ocean fronts. *Ocean Modelling* 14:241–256, http://dx.doi.org/10.1016/j.ocemod.2006.05.006.

Taylor, J.R., and R. Ferrari. 2009. On the equilibrium of a symmetrically unstable front via a secondary shear instability. *Journal of Fluid Mechanics* 622:103–113, http://dx.doi.org/10.1017/S0022112008005272.

Taylor, J.R., and R. Ferrari. 2010. Buoyancy and wind-driven convection at mixed layer density fronts. *Journal of Physical Oceanography* 40:1,222–1,242.

Thomas, L.N. 2008. Formation of intra-thermocline eddies at ocean fronts by wind-driven destruction of potential vorticity. *Dynamics of Atmospheres and Oceans* 45:252–273, http://dx.doi.org/10.1016/j.dynatmoce.2008.02.002.

Thomas, L.N., J.R. Taylor, R. Ferrari, and T.M. Joyce. 2013. Symmetric instability in the Gulf Stream. *Deep Sea Research Part II* 91:96–110, http://dx.doi.org/10.1016/j.dsr2.2013.02.025.

Vinaychandran, P.N., V.S.N. Murthy, and V. Ramesh Babu. 2002. Observations of barrier layer formation in the Bay of Bengal during summer monsoon. *Journal of Geophysical Research* 107(C12):1–9, http://dx.doi.org/10.1029/2001JC000831.

Weller, R.A., J.T. Farrar, J. Buckley, S. Mathew, R. Venkatesan, J. Sree Lekha, D. Chaudhuri, N. Suresh Kumar, and B. Praveen Kumar. 2016. Air-sea interaction in the Bay of Bengal. *Oceanography* 29(2):28–37, http://dx.doi.org/10.5670/oceanog.2016.36.

ACKNOWLEDGMENTS

We appreciate financial support under the ASIRI initiative from the Office of Naval Research and under the OMM initiative of India's Monsoon Mission supported by the Ministry of Earth Sciences, New Delhi. Figure 6 was generated with assistance from Caroline Stjärnborg.

AUTHORS

Sutanu Sarkar (sarkar@ucsd.edu) is Blasker Professor, Department of Mechanical and Aerospace Engineering, and Affiliate Professor, Scripps Institution of Oceanography, University of California, San Diego, La Jolla, CA, USA. **Hieu T. Pham** is Assistant Project Scientist, Department of Mechanical and Aerospace Engineering, University of California, San Diego, La Jolla, CA, USA. **Sanjiv Ramachandran** is Research Associate, Department of Mechanical Engineering, University of Massachusetts Dartmouth, North Dartmouth, MA, USA. **Jonathan D. Nash** is Professor, College of Earth, Ocean, and Atmospheric Sciences, Oregon State University, Corvallis, OR, USA. **Amit Tandon** is Professor of Mechanical Engineering, and **Jared Buckley** is a graduate student, University of Massachusetts Dartmouth, North Dartmouth, MA, USA. **Aneesh A. Lotliker** is Scientist, Indian National Centre for Ocean Information Services, Hyderabad, India. **Melissa M. Omand** is Assistant Professor, Graduate School of Oceanography, University of Rhode Island, Narragansett, RI, USA.

ARTICLE CITATION

Sarkar, S., H.T. Pham, S. Ramachandran, J.D. Nash, A. Tandon, J. Buckley, A.A. Lotliker, and M.M. Omand. 2016. The interplay between submesoscale instabilities and turbulence in the surface layer of the Bay of Bengal. *Oceanography* 29(2):146–157, http://dx.doi.org/10.5670/oceanog.2016.47.